Experimental and Theoretical Study for Evaluating Journal Bearing Performance under Internal Combustion Engine Operating Conditions Using Mixed Simulation Methodology

Studi Eksperimental dan Teoretis untuk Mengevaluasi Kinerja Bantalan Jurnal pada Kondisi Operasi Mesin Pembakaran Dalam Menggunakan Metodologi Simulasi Campuran

Kabas Aziz Hassan[1], Mariya Thaer Abdulhadi[2], Shuhub Ahmed Shihab[3]
ms.c.kabasa.hassan@mtu.edu.iq[1], mariya.thaer@ibnsina.edu.iqv[2],
shuhub.ahmed@uoturath.edu.iq[3]

[1] Middle technical University , Anbar Technical Institute Iraq
[2] Ibn Sina University of Medical and Pharmaceutical Sciences, Baghdad, Iraq
[3] AL-Turath University, Iraq

Abstrak

Latar Belakang Umum Mesin pembakaran dalam modern menuntut efisiensi tinggi dan ketahanan operasional di bawah tekanan termal dan mekanis yang ekstrem. Latar Belakang Khusus Bantalan jurnal sering beroperasi di bawah beban ekstrem, yang beralih dari režim pelumasan hidrodinamik ke režim pelumasan campuran. Kesenjangan Pengetahuan Namun, memprediksi kerugian gesekan tetap menjadi tantangan karena interaksi kompleks antara deformasi permukaan elastis, piezoviskositas, dan pengenceran geser. Tujuan Penelitian ini menyajikan metodologi terintegrasi yang menggabungkan evaluasi rig uji eksperimental dengan simulasi hidroelastis multi-badan untuk mengevaluasi kinerja bantalan jurnal. Hasil Hasil menunjukkan bahwa meskipun suhu menurunkan viskositas oli, tekanan hidrodinamik tinggi yang melebihi 200 MPa justru meningkatkan viskositas, sedangkan laju geser hingga $2{,}2\times10^{7}$ s^{-1} menyebabkan pengenceran geser yang nyata pada kecepatan tinggi. Selain itu, tegangan kontak tepi awal menurun dengan cepat selama fase pemakaian awal. Inovasi Kerangka kerja termo-elasto-hidrodinamika yang sepenuhnya terintegrasi dan memasukkan topografi permukaan yang aus telah dikembangkan. Implikasi Wawasan ini memungkinkan desain geometri bantalan yang dioptimalkan dan formulasi pelumas canggih untuk mesin dengan efisiensi tinggi.

Kata kunci: Bantalan Jurnal, Pelumasan Campuran, Elastohidrodinamika, Torsi Gesekan, Mesin Pembakaran Dalam

Abstract

General Background Modern internal combustion engines demand high efficiency and operational durability under severe thermal and mechanical stresses. Specific Background Journal bearings frequently operate under severe loading, transitioning from hydrodynamic to mixed lubrication regimes. Knowledge Gap However, predicting frictional losses remains challenging due to complex interactions between elastic surface deformations, piezoviscosity, and shear thinning. Aims This study presents an integrated methodology combining experimental test-rig evaluations with multi-body hydroelastic simulations to evaluate journal bearing performance. Results Results indicate that while temperature reduces oil viscosity, high hydrodynamic pressures exceeding 200 MPa increase viscosity, whereas shear rates up to 2.2×10^{7} s^{-1} cause noticeable shear thinning at high *speeds. Additionally, initial edge contact stresses decrease rapidly during the running-in phase. Novelty A fully coupled thermo-elasto-hydrodynamic framework incorporating worn surface topographies is established. Implications These insights enable optimized bearing geometry designs and advanced lubricant formulations for high-efficiency engines.*

Keywords : Journal Bearings, Mixed Lubrication, Elastohydrodynamics, Friction Torque, Internal Combustion Engines

Introduction

Studying the performance of sliding bearings in internal combustion engines is critical due to the high loads and harsh operational environments they endure, while traditionally relying on hydrodynamic lubrication, the drive for improved engine efficiency and reduced emissions has pushed the transition towards mixed lubrication regimes. However, this transition poses significant durability challenges, as partial metal-to-metal contact increases the risk of wear, therefore, this study presents an integrated methodology [1-2], combining theoretical simulation and experimentation, to comprehensively evaluate sliding bearing performance under these demanding conditions, the theoretical approach utilizes an elastohydrodynamic lubrication (EHL) model [5] to analyze pressure distribution and surface deformations, while a series of carefully designed experiments [3-4] investigate the effects of varying speed, temperature, and load on key performance metrics, through this dual approach, the study aims to elucidate the complex relationship between operating parameters and the transition to mixed lubrication [6], providing critical insights for the development of innovative lubricants and advanced bearing designs that enhance durability and efficiency in internal combustion engines [7].

Reference study

The design of sliding bearings in modern internal combustion engines is confronted with a multitude of challenges driven by continuous technological advancements aimed at increasing performance and fuel efficiency. A primary challenge arises from engine downsizing and turbocharging, which create high power densities that escalate thermal and mechanical loads, this requires bearings to withstand extreme pressures, often exceeding 100 MPa, while maintaining a lubricant film that can shrink to less than a micron, significantly increasing the risk of detrimental metal-to-metal contact [8].

Further complicating performance are start-stop systems, which impose frequent mixed lubrication cycles during engine restarts, this repeated operation accelerates wear due to increased friction, a challenge explored in the pivotal work of Mokhtar et al. (1977) on the wear characteristics of bearings under repetitive conditions [9]. Similarly, cylinder deactivation technology, while improving fuel economy, fundamentally alters crankshaft dynamics and introduces additional shaft deformations. Studies by Wilcutts et al. (2013) and Mohammadpour et al. (2014) highlighted these changes in load dynamics, while Shahmohamadi et al. (2015) investigated the resulting thermal effects, such as cavitation, which can increase frictional losses and long-term wear.

The widespread adoption of low-viscosity lubricants, advocated by Holmberg et al. (2014) to reduce parasitic energy losses, creates another critical design trade-off, while beneficial for efficiency, these oils can compromise the integrity of the hydrodynamic film, potentially leading to accelerated wear under heavy loads, as demonstrated in the work of Macián et al. (2014, 2016), the complex non-Newtonian properties of modern lubricants, particularly the piezo-viscous effect at high shear rates, further complicate performance prediction and necessitate the use of advanced simulation models, such as the comprehensive one developed by Allmaier et al. (2012) [10-11].

In response to these multifaceted challenges, advanced technologies like surface texturing and protective coatings are being deployed. Research by Ligier et al. (2015), for instance, has shown the effectiveness of materials like Diamond-Like Carbon (DLC) coatings in enhancing wear resistance and improving bearing reliability under harsh conditions, this research builds upon this foundation by combining experimental analysis and theoretical simulation to achieve a deeper understanding of bearing behavior, aiming to develop robust solutions that enhance the efficiency, reliability, and durability of modern internal combustion engines.

Experience:

Simulating the performance of hydrodynamic sliding bearings requires careful evaluations of operational properties and elasticity to keep up with current challenges in internal combustion engines, especially with increasing mechanical loads in small turbocharged engines, which causes elastic deformations of engine parts that require taking this elastic deformation into account within the simulation[12] and such as elastic deformation of the shaft may cause a mismatch between the sliding bearing and the shaft, affecting the bearing behavior. At the same time, high pressure in the contact areas leads to local surface deformation that affects the thickness of the lubricating film, which increases the importance of taking into account the elasticity of the bearing shell, which is usually weaker than the hardened shaft and the importance of the rheological properties of oils used under high pressure is highlighted, as the viscosity of the oils increases[12] and in these cases significantly, which is known as the piezoviscosity effect and the effectiveness of the viscosity inside the lubrication gap changes significantly caused by differences in hydrodynamic pressures and local shear rates, and these changes play a major role in determining the behavior of the bearing under varying loads and operating conditions and as the lubricant film thickness decreases under mixed lubrication conditions, the prediction of metal-to-metal contact becomes critical, requiring accurate models to describe this contact in the simulation of bearing wear behavior. Simulation also requires an accurate representation of the surface structure of the bearing, both in terms of physical composition and surface topography. Modern bearings are increasingly operating in mixed lubrication environments, and with advances in surface properties [13], it is essential that the parameters used in the simulation are based on actual surface measurements. Any deviation between the bearing and the shaft can result in sharp metal-to-metal contact, especially at the bearing edges and the bearing skin can adapt during initial operation to provide a better match with the shaft and these morphological surface modifications may exceed the minimum lubrication gap, which means they must be taken into account to avoid overestimation of metal contact. Since dynamic sliding bearings are subject to time-varying loads, the non-linear behavior of the bearings requires transient dynamic calculations to arrive at accurate results, especially When studying the bearing behavior during frequent start and stop phases and thermal effects also affect the viscosity of lubricating oils and should be included in the simulation and the model in this study is based on temperatures equivalent to isothermal simulations, but local thermal changes need to be studied in detail in the future to develop more accurate models[14] and the simulation of mixed hydrodynamic elastomeric lubrication combines two main principles, the Reynolds equation and equations describing friction and wear in shaft bearings and the Reynolds equation is fundamental to understanding the lubricant film in axle bearings, which governs the flow of oil between opposing surfaces. As the distance between these surfaces' decreases, the surface roughness becomes more influential on the lubricant flow and to illustrate this, Pater and Cheng introduced flow factors that modify the Reynolds equation, allowing it to incorporate both hydrodynamic pressure and lubricant film thickness and these factors are adjusted for both the axial and circumferential directions and depend on the sliding velocities of the surfaces and surface roughness is represented in the model by pressure flow factors for the axial and circumferential directions, while the shear flow factor models the effect of pressure on the lubricant's viscosity and the viscosity itself is affected by key variables such as temperature, pressure, and shear rate, all of which play crucial roles in the behavior of the bearing and the model also simulates the eventual breakdown of the lubricant film, which may fail to keep the surfaces fully separated, causing direct metal-to-metal contact, when this occurs, the (Greenwood and Tripp) contact model is applied to calculate the contact pressure, taking into account the composite elastic modulus of the contacting surfaces and this model also factors in an elasticity term that considers surface roughness, asperity radius, asperity density, and a shape factor that accounts for the gap size between the surfaces.

When determining frictional losses in heavily loaded journal bearings, these losses arise either from hydrodynamic effects alone or from a combination of hydrodynamic and metal-to-metal contact losses and the total friction torque is calculated by integrating the shear stresses from both sources across the bearing surface. Hydrodynamic shear stress is determined by factors such as sliding velocity, pressure, and film thickness, while shear stress from metal contact is calculated by multiplying the contact pressure by the boundary friction coefficient and these equations provide a comprehensive understanding of the friction behavior in the system. [17]:

$$\frac{\{\partial\}}{\{\partial x\}}\left(\frac{\{\partial h\}}{\{\partial x\}}+\frac{\{\partial h\}}{\{\partial y\}}+\frac{\{\partial h\}}{\{\partial t\}}\right)-\frac{\{h\}}{\{s\}}=\ 0 \quad (1)$$

Equation (1) represents the oil flow using flow factors in different directions. For hydrodynamic losses, the shear stress is calculated using the equation:

$$\tau_h = \frac{\{u_1 u_2\}}{\{h\}} \, (2)$$

Equation (2) is used to calculate the hydrodynamic shear stress, where it depends on the sliding velocities and pressure in the lubricant gap. Finally, the asperity shear stress from metal-to-metal contact is calculated using the equation [18]:

$$F_a = \ K \ \cdot E^{*} \cdot F^{\left\{\frac{5}{2}\right\}} \quad (3)$$

Equation (3) represents the metal-to-metal contact between the surfaces when the lubricant film does not fully separate them, with the contact pressure depending on the composite elastic modulus and the contact area between the surfaces and based on these equations, the friction torque is calculated using the following formula:

$$M_{\{\{friction\}\}} = \ \int_{,}\{\{A\}\}(\tau_h + \ \tau_a)dx\,, dy \quad (4)$$

Equation (4) expresses the total friction, including both the hydrodynamic shear stress and the friction resulting from asperity contact in metal-to-metal interactions [19].

Lubricant Behavior Under High Pressure and Shear Conditions

This study employed a fully formulated, low-viscosity, 0W-20 hydrocarbon engine oil as the lubricant, this multi-grade lubricant is commonly used and readily available in the automotive market, the essential properties of this lubricant are detailed in Table1.

Table 1: Fundamental Properties of the 0W-20 Lubricant Tested

Property	Value
Density at 40°C	833.6 kg/m³
Dynamic Viscosity at 40°C	36.9 mPa·s
Dynamic Viscosity at 100°C	6.98 mPa·s
HTHS-viscosity at 150°C and shear rate of 10^6 1/s	2.68 mPa·s

The properties of the lubricant indicate that the viscosity is highly affected by temperature. Various mathematical models can be used to simulate this temperature-dependent behavior and in this study, the **Vogel equation** is utilized to elucidate the effect of temperature on viscosity, as it provides an accurate representation for hydrocarbon-based lubricants [20]:

$$h\,(T) = A \cdot e^{(T+CB)} \quad (5)$$

Where: - T is the oil Temperature in °C.

- A, B, and C are constants that are specific to the lubricant.

High stresses, which may exceed 200 A, occur within dynamically loaded axle bearings. leading to a significant increase in viscosity and this increase in viscosity due to pressure is modeled using the **Barus equation**:

$$h(T,p) = h(T) \cdot e^{\alpha p} \quad (6)$$

Where:

- $h(T,p,\gamma^{\cdot})$is the viscosity at temperature T and pressure p,
- α is the pressure-viscosity coefficient (1/bar).

The shear rates in journal bearings can exceed 2×1072 \times 10^72×107 1/s under high load and speed conditions, leading to a noticeable reduction in viscosity, known as **shear thinning** and to model this shear thinning effect, the **Cross equation** is used:

$$h(T,p,\gamma^{\cdot}) = \frac{h(T,p)}{1 + K.\gamma^{\cdot}} \quad (7)$$

Where:

- $h(T,p,\gamma^{\cdot})$is the viscosity at temperature T, pressure p, and shear rate $\gamma^{\cdot}$
- $\gamma^{\cdot}$ is the shear rate,
- K, r, and mmm are empirical coefficients for the lubricant [21].

The rheological parameters obtained from the measured data for the lubricant are shown in Table

2.

Table 2: Rheological Model Parameters for the Lubricant.

Parameter	Value
A	0.05177 mPa·s
B	1135.6°C
C	132.1°C
α	0.00088 1/bar
r	0.531
m	0.81
K	7.9×10^{-8} s

The viscosity characteristics for the lubricant, derived from the above parameters, are also shown in Figures1 and 2 These figures illustrate how viscosity changes under different temperature, pressure, and shear rate conditions and the experimental data are extensively used to validate the simulation approach presented in this study and although this paper does not primarily focus on the experimental setup, a short description of the journal bearing test rig is provided. Further details on the test rig and the measurement devices used are available in the references. All tests were performed on the journal bearing test rig at KS Gleitlager as depicted in Figure 3 and this rig facilitates a comprehensive examination of journal bearing behavior under various static and dynamic loading conditions, with the flexibility to test at both constant and varying shaft speeds.

The rig is designed with a straight test shaft supported by two brackets, each one contains a journal bearing mounted on a stable base, as well as a test bearing, A test bearing is positioned on a connecting rod between support bearings. A load is applied to the test bearing through an electromechanical high-frequency pulsator while an electric motor equipped with an elastic coupling drives the shaft and support bearings, which are designed with a 180° oil supply groove, are representative of those used in automotive main bearings and they feature a diameter of 54 mm and a width of 25 mm. In comparison, the test journal bearing, similar to a big-end bearing, has a diameter of 47.8 mm and a width of 17.2 mm [22].

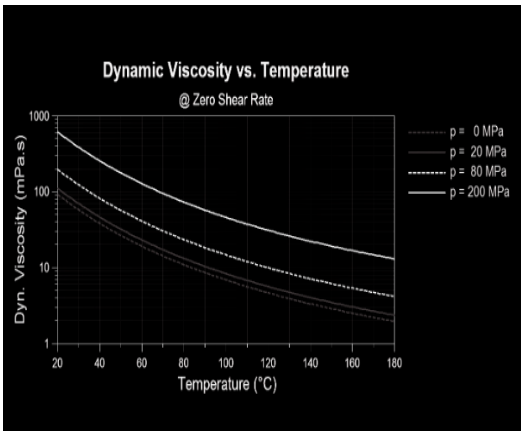

Figure 1. Temperature dependence of viscosity of lubricant 0W20 at different pressures

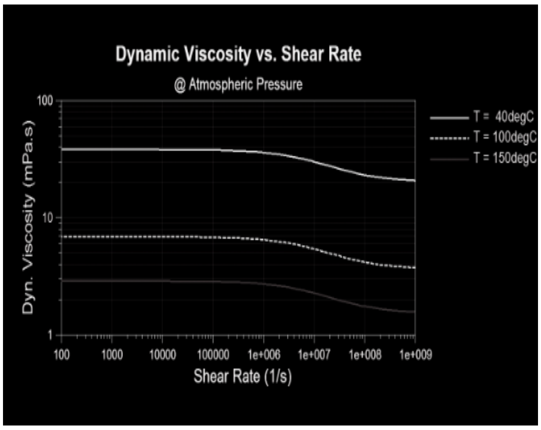

Figure 2. Shear viscosity dependence for 0W20 lubricating oils at different temperatures

A torque transducer positioned between the motor and the clutch measures the total friction torque generated by the three journal bearings, providing an accurate assessment of the torque generated during operation. For the purpose of simulation, the test rig is modeled using the flexible multi-body dynamics solver AVL Excite Power Unit and this solver accommodates both flexible components and the joints that connect these components, as well as the support brackets and bearings and to represent the journal bearings in the simulation, both the test bearing and the support bearings are modeled as condensed finite element (FE) structures and to create these simplified FE representations, a preprocessing step using an FE solver is necessary and in contrast to the condensed FE approach used for the bearings, the test shaft is modeled as an elastic body. Instead of representing it as a condensed FE structure, the shaft is simplified to a combination of beam and disc geometries, which are computationally less intensive yet still accurately capture the system's behavior and the lubrication interactions between the test shaft and both the support bearings and the test bearing are modeled as elasto-hydrodynamic joints, which accounts for the lubricated contact under varying pressure and shear conditions and the fluid film characteristics within these joints are determined using the Reynolds equation, as outlined earlier, to calculate the lubrication film behavior between the contacting surfaces and in order to solve the complex behavior of the bearing system, the bearing surfaces are discretized into smaller segments, referred to as nodes. For each bearing, the axial direction is discretized into 25 hydrodynamic (HD) nodes, with an equal distribution of these nodes between the test bearing and the support bearings, the test bearing is modeled with 200 nodes in the circumferential direction, while the support bearings are represented by 176 nodes and this level of discretization ensures that the simulation captures the detailed variations in the fluid film and bearing behavior. Additionally, every other HD node is directly coupled to the condensed FE model, providing a more accurate representation of the bearing system's dynamics and due to the highly nonlinear nature of the system, the simulation is solved in the time domain, using numerical time integration methods and this approach allows for capturing transient effects and dynamic behaviors in the bearing system over time and the nonlinearity arises from the complex interaction of various factors such as pressure distribution, lubrication conditions, and surface interactions, making time-domain analysis essential for accurately predicting the system’s performance under operational conditions and this simulation setup provides a robust framework for analyzing the behavior of journal bearings, including their frictional characteristics, under a range of loading and lubrication scenarios [23-24].

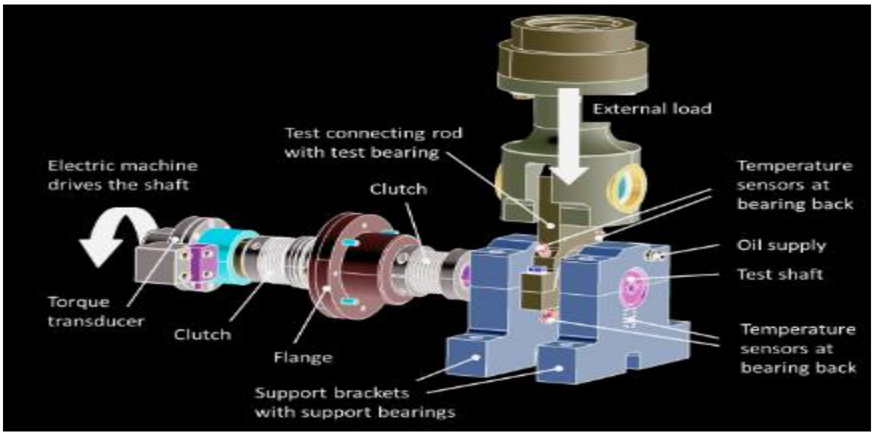

Figure 3: Configuration and Components of the Axle Bearing Test Rig

In the isothermal simulation method, it is assumed that both the temperature of the bearing and the lubricant remains constant within the lubrication gap and although temperature fluctuations due to changing operational conditions—such as variations in shaft speed and bearing load—are expected, these changes are addressed in the simulation by using an equivalent temperature and this temperature is derived from real-time measurements taken from the back of the bearing shell, as outlined in the test-rig schematic Figure 3 and this approach is based on prior work by Allmaier et al., who studied thermal behavior in journal bearings under dynamic loading, they compared their findings with experimental data and the research by Allmaier and colleagues demonstrated that the temperature at the bearing shell could be accurately predicted using a complex thermo-elasto-hydrodynamic (TEHD) model, which combines temperature, pressure, and lubrication effects, building upon these findings, a simplified formula was developed to estimate the equivalent bearing temperature, which can be used for isothermal simulations and this method still incorporates the temperature variations induced by different operating conditions but does so in a way that avoids the need for a more complex TEHD simulation and the simplified method enables predictions of friction losses in bearings under a wide variety of operating conditions and with different types of lubricants, shaft speeds, and loads and this method has been validated through direct comparison with experimental results, showing its accuracy in estimating frictional losses. Initially developed for bearings with distinct oil supply grooves, which direct the lubricant to the bearing surface, this method has since been adapted for bearings that use oil supply holes, making it suitable for different types of bearing designs and by using this simplified equivalent temperature method, engineers can simulate thermal influences on bearing performance more efficiently and this provides a practical solution for predicting friction and wear in bearings across various operating conditions without the computational intensity of full thermal simulations. [25-26]

Result:

When investigating the performance of sliding bearings under various operating conditions, both elastic deformation of bearing surfaces and changes in lubricant viscosity due to high pressure and shear rate must be taken into account. especially when subjected to dynamic loads while operating within a hydrodynamic elastic lubrication system and to achieve accurate predictions of friction and wear, when bearings are subjected to constant load and low shaft speed, metal-to-metal contact becomes important, providing an opportunity to validate the simulation model under mixed lubrication conditions and the results presented here are derived from recent research by the authors, with further details available in previous work. In addition, the effect of high pressure and low viscosity on friction in dynamic sliding bearings is discussed, with the bearings operating in a hydrodynamic elasto-lubrication environment. Under heavy loads, hydrodynamic pressures can exceed 200 MPa, while at shaft speeds up to 7000 rpm, the lubricant is subjected to significant shear, which reduces its viscosity and this analysis emphasizes the importance of accurately modeling the behavior of lubricants under such extreme conditions to make an accurate prediction, friction and the study also highlights how neglecting the impact of compressive viscosity and Non-Newtonian behavior can lead to errors when predicting friction in sliding bearings and two different dynamic load scenarios were tested: he first with a peak external load of 40 (kN) and the second with a higher load of 80 (kN) and the load characteristics during the full cycle are depicted in Figure 4 and the results reveal that high pressure increases the viscosity of the lubricant, primarily due to the compressive viscosity effect, which is critical for maintaining the lubricant film under heavy loads. However, as the shaft speed increases, viscosity thinning occurs, reducing the ability of the lubricant to maintain an adequate film thickness, leading to increased friction and wear and these trends are consistent with theoretical predictions, confirming the accuracy of the simulation model and emphasizing the need to consider viscosity changes when predicting the behavior of sliding bearings under dynamic loading conditions and figure 4 also presents the time-dependent variations of the load applied to the bearing and the cyclic loads, which fluctuate within a specified range, simulate the real operating conditions encountered by sliding bearings in industrial environments, by analyzing these cycles, the effect of varying loads on bearing performance and lubricant film thickness can be studied in more detail.

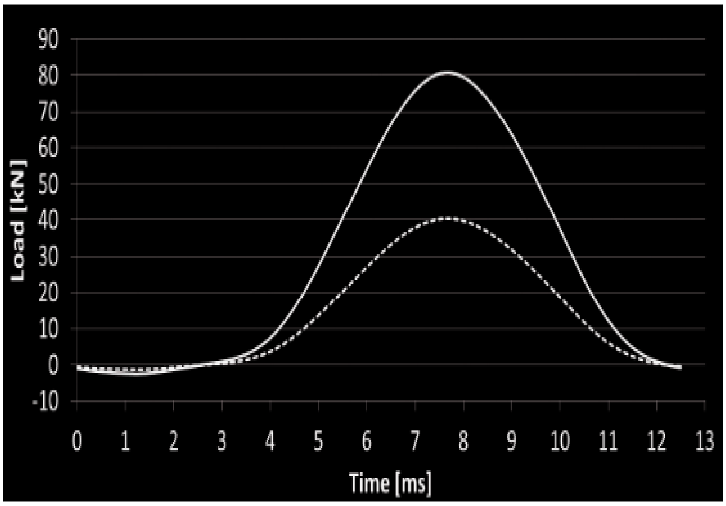

Figure 4. Variation of dynamic load on the test bearing

This study aims to assess the dynamic performance of a sliding bearing under varying load conditions and rotational speeds. Specifically, the bearing is subjected to maximum specific loads, which are determined by the projected bearing area and the applied loads correspond to 50 MPa for a 40 kN load and 100 MPa for an 80 kN load and the shaft speed begins at 1000 rpm, then gradually increases in increments of 1000 rpm until reaching a maximum of 7000 rpm, with each speed step being maintained for a duration of 20 minutes. Once the maximum speed is achieved, the shaft speed is gradually decreased back to 1000 rpm and these operating conditions closely replicate the dynamic environment found in internal combustion engines and to validate the simulation, the results are compared with experimental data that measure the friction torque behavior in the sliding bearing and to simulate this behavior accurately, three distinct lubrication models are employed and these models are selected to reflect various lubrication scenarios within the flexible sliding lubrication system and the results are analyzed to examine the impact of lubricant properties on the accuracy of the simulation outcomes, by doing so, the study highlights the importance of accurately modeling lubrication properties in predicting the dynamic performance of sliding bearings under real-world operating conditions.

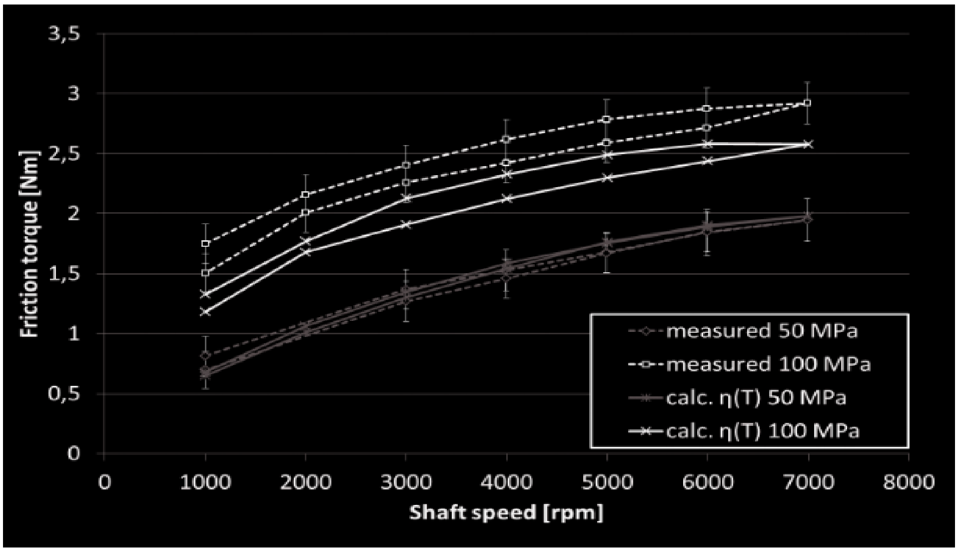

Figure 5. Comparison of Average Frictional Torque Measured on Test Bench and Average Torque Simulated Using Base Oil Model η(T) at Specified Loads of 50 and 100 MPa

The study begins by evaluating different lubrication models to understand their influence on the friction torque in sliding bearings and the simplest model is based solely on temperature-dependent viscosity, denoted as η(T), which represents how viscosity changes with temperature. Subsequently, the model is expanded to include the effect of pressure, resulting in the model $\eta(T, p)$, which accounts for both temperature and pressure effects on the lubricant. Finally, a more comprehensive model is adopted, incorporating the shear softening effect, denoted as $\eta(T, p, \gamma)$, which takes into account the shear rate's impact on lubricant viscosity and figure 5 presents a comparison between the friction torque measured experimentally in the test rig and the friction torque calculated using the basic lubrication model η(T), under two specific load conditions: 50 MPa and 100 MPa and the measured friction torque data is represented by dashed lines, and error bars are included to reflect the uncertainty in the measurements, such as the torque converter error and the mean's standard error. As anticipated, the friction torque increases as the shaft rotational speed and the load increase and the effect of temperature on friction is evident, particularly when comparing the friction torque results under a 100 MPa load during both the speed-up and slow-down phases. In the second phase, when the bearing temperature rises by approximately 3°C, there is a noticeable decrease in the friction torque by around 0.2 Nm and this reduction is due to the decrease in viscosity at the higher temperatures, as the oil becomes less resistant to flow and the η(T) model, which accounts only for temperature-induced viscosity changes, is represented by the solid line in Figure 5. It shows a strong agreement with the measured friction torque at a load of 50 MPa, indicating that temperature effects alone can be accurately captured in the model for this load condition. However, at a load of 100 MPa, the calculated friction torque values were consistently lower than the measured values across the entire range of shaft speeds and this discrepancy highlights the influence of additional factors, such as pressure, on the viscosity at higher loads, which the simple temperature-only model cannot fully account for and the temperature rise observed during the idle phase was correctly predicted by the model, confirming that the isothermal bearing assumptions work as expected and the simulation results also produced valuable results regarding the formation of the oil film and the resulting hydrodynamic pressures within the bearing. For instance, under a 100 MPa load, the peak oil pressure was found to reach approximately 200 MPa, regardless of the shaft speed.

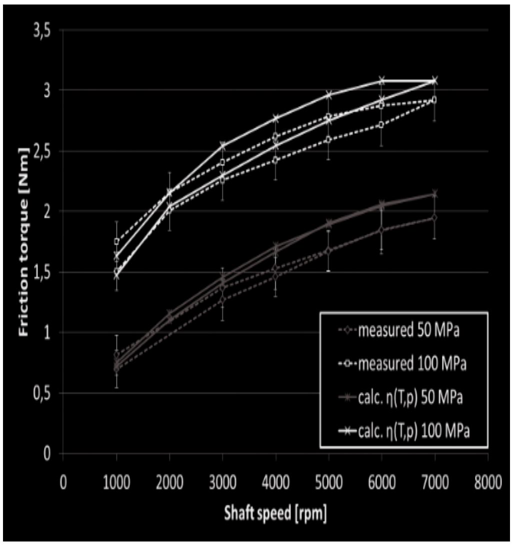

Figure 6. Comparison of Average Friction Torque Measured on the Test Rig and Average Torque Simulated Using the Pressure-Dependent Oil Model η(T,p) at Specific Loads of 50 and 100 MPa

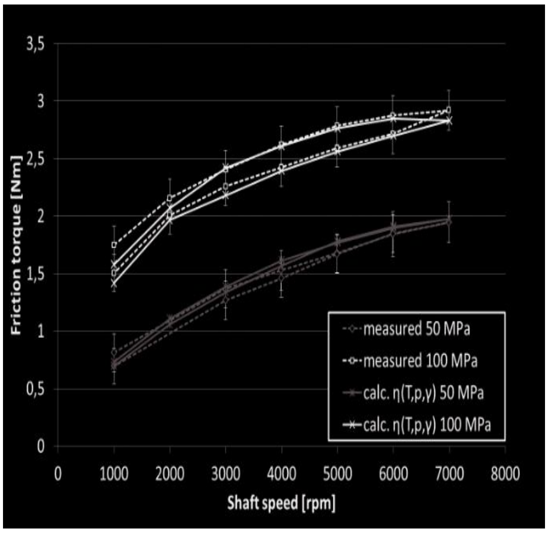

Figure 7. Comparison of Average Friction Torque Measured on the Test Rig with Average Friction Torque Simulated Using the Full Oil Model η(T,p,γ;.) at Specific Loads of 50 and 100 MPa

This demonstrates the significant pressure that develops in the bearing, highlighting the importance of considering pressure effects when modeling lubrication behavior and in the next stage, the model $\eta(T,p)$ that includes the effect of pressure on lubricant viscosity is employed. Figure 6 illustrates how the inclusion of pressure in the model leads to an increase in the friction torque under all operating conditions and this model has a more pronounced effect under higher load conditions, such as 100 MPa, where the friction torque increases further compared to the simpler η(T) model and this reflects the complex relationship between pressure, temperature, and viscosity in high-load bearing operations, where both temperature and pressure significantly influence the lubricant's performance and at low shaft speeds, the calculated values were consistent with the measured values of friction torque for both cases, but as the shaft speed increased above 3000 rpm, the calculated torque significantly exceeded the measured values and as the shaft speed increased, the shear rates increased almost linearly, reaching the maximum value is 2.2 x 10^7 1/s at a speed of 7000 rpm, which leads to a decrease in oil viscosity due to the shear reduction effect by up to 25% according to Figure 2. Accordingly, the full model that takes into account temperature, pressure and shear effect ($\eta(T,p,\gamma)$) was used, and its results are shown in Figure 7. At low speeds, the reduction effect due to shear is Insignificant, but becomes more noticeable at high speeds, as it leads to a reduction in the calculated friction torque, especially at shaft speeds exceeding 5,000 RPM, with a torque variation of approximately 0.15 Nm between Both models, regardless of load status.

Edge stress and wear in dynamically loaded journal bearings during the running-in period.

Archard's wear equation is used to calculate the wear depth based on the factors affecting the wear process between two contacting surfaces and the equation expresses the relationship between the load and the relative hardness of the two contacting surfaces, where the wear depth at each point of contact is determined based on several variables and the basic formula for Archard's wear equation is:

$$h_W = W \cdot L \cdot \frac{C}{H}$$

Where:

h_W: Wear depth at the specified location (wear depth).

W: Normal load applied to the surface (normal load).

L: Sliding distance between the two surfaces (sliding distance).

C: Wear coefficient, which expresses the ease of wear and depends on the properties of the materials in contact.

H: hardness of the contact surface, which is a key factor in determining the resistance of the material to wear.

This equation is applied to each point of the connected surface that has been divided into nodes, where the load is calculated and the wear is estimated at each node. After that, these calculations are repeated for each time step, so that the shape of the bearing surface is gradually updated, which allows modeling the effect of wear on the general shape of the worn surface and this iterative method is used in simulation to update the geometric shape of the bearing as the wear increases and the iterative process continues until a state is reached and the impact of wear is significantly reduced, which allows understanding the gradual development of wear on the bearing surface and analyzing its effect under different operating conditions and figure 8 is intended to simulate the “running-in” process, which occurs when surfaces in contact begin to adapt to each other by removing a small surface layer to reduce metal contact.

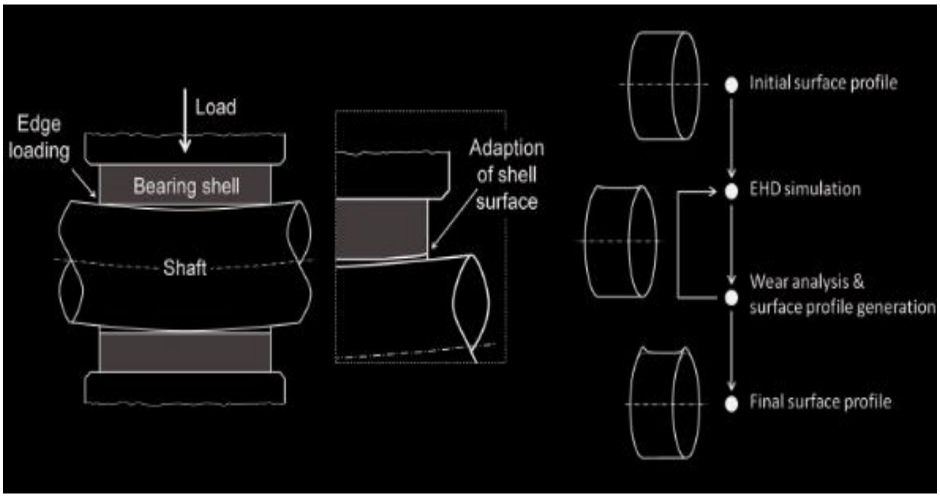

Figure 8. Edge Loading Due to Elastic Bending of the Column
Flow Chart for Generating the Iterative Surface Profile on the Right

When dynamic bearing friction tests were performed, it was found that there was significant wear at the bearing edges and the simulation was based on considering these areas as worn from the beginning rather than assuming an ideal cylindrical bearing surface and the Archard wear equation was used to calculate the wear depth incrementally, where the depth is determined by the normal force, sliding distance, wear coefficient, and surface hardness and this approach creates a new bearing surface profile, and the simulation process is repeated for each step until the metal-to-metal contact stress becomes insignificant. At the start of the test, the shaft speed was set at 4,000 RPM with a load of 100 MPa, the test showed significant metal-to-metal contact at the bearing edges, due to the symmetrical distribution of stresses resulting from the elastic bending of the shaft under load and as shown in Figure 9 and the metal-to-metal contact stress is distributed symmetrically on both sides of the edges and the figure also shows how the maximum pressure changes over successive simulation steps, with the pressure value gradually decreasing at the beginning and then slowing down as the steps increase and as part of the process, the wear depth is determined at each step at the point with the maximum load on the bearing surface, and the wear depth at the remaining points is calculated based on the distribution of the stress resulting from the loading and after the bearing surface is updated according to this wear, another full hydrodynamic loading simulation is started, and this iterative process continues until the metal-metal contact resulting from the surface wear is no longer significant. Figure 10 illustrates the evolution of the surface morphology in the bearing, showing that the wear is mainly concentrated at the upper bearing edges, and as the steps increase, the wear extends to cover a larger area of the axial and circumferential surfaces, and the wear depth reaches 3.6 μm after 40 simulation steps. Figure 11 shows a rapid decrease in the metal-metal contact pressure at the beginning, reaching below 5 MPa during the first 200 s, and then gradually decreasing to the end. Additionally, wear volume increases sharply at the beginning and gradually stabilizes as time passes.

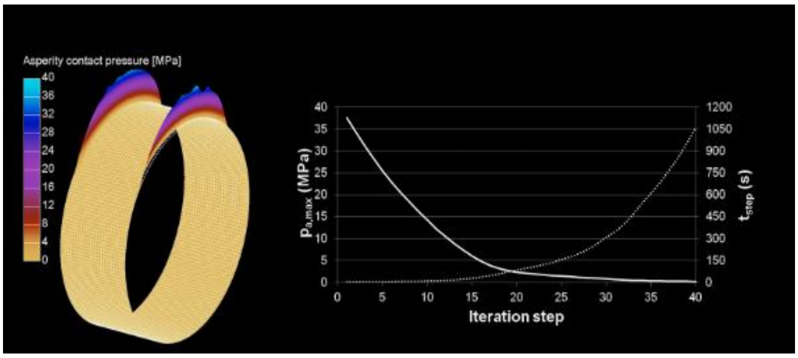

Figure 9. Computed contact pressure at the maximum load point during the first step on the left development of the maximum extreme contact pressure and step time as a function of the number of iterative steps.

The process illustrates the effect of “run-in” or “run-in” on the bearing surfaces; the surface is naturally adjusted to accommodate the high friction caused by metal-to-metal contact at the beginning of operation and this metal-to-metal contact was confirmed in the experiment to be more pronounced in the early steps, which explains why the friction torque differs between the measured and calculated values in the low-speed tests, and is also due to additional friction caused by metal wear that was not predicted in the simulation due to the use of an already worn surface and this study shows that the run-in process is concentrated in small areas on the bearing surface and results in limited metal-to-metal contact, which has little impact on the overall friction losses in the bearing.

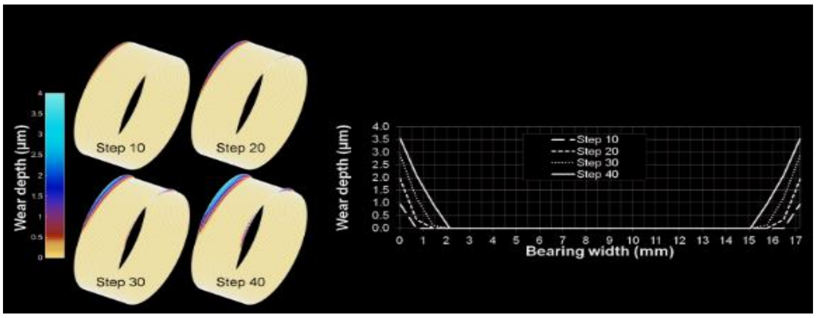

Figure 10. Surface profile on the left and a sectional view of the surface profile at the location of maximum wear depth during the iterative manufacturing process on the right.

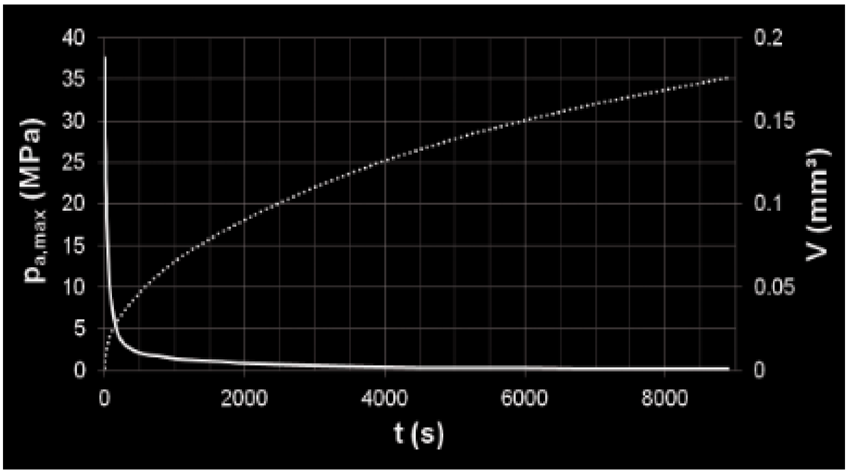

Figure 11. Maximum contact pressure and accumulated wear volume as a function of time.

The study investigates the behavior of journal bearings under mixed lubrication conditions, where metal-to-metal contact occurs due to high loads or low lubrication film thickness and this metal-to-metal contact significantly influences the friction in the bearing, making surface roughness and texture critical factors in predicting friction and wear, the bearing surface is represented in the simulation model using the Greenwood and Tripp contact model, which accurately predicts the contact pressure and the contact area during metal-to-metal interaction and the model assumes a constant friction coefficient, and the simulation is validated using surface scan data from the bearing to ensure that the effects of surface roughness are properly accounted for and to simulate and validate the occurrence of metal-to-metal contact, the experiments involved applying a constant load to the bearings and the tests began at high shaft speeds, which were gradually reduced to enter the mixed lubrication regime, where both hydrodynamic and boundary lubrication conditions exist simultaneously and the results were analyzed using Stribeck curves, which illustrate the relationship between friction torque and shaft speed, helping identify different lubrication regimes. Two load conditions were tested: one at a constant load of 8 kN (specific pressure of 10 MPa) and another at 4 kN (5 MPa). In each test, new bearing shells were installed, and the shaft speed was increased gradually to 6000 rpm before decelerating to zero and the test duration was about 12 minutes, with only the deceleration phase being recorded and analyzed and before and after each test, the bearing surface was scanned using a white light interferometer to measure surface roughness and the roughness of the new bearings had an arithmetic mean roughness (R_a) of 0.27 μm, which decreased to 0.22 μm after the test, indicating wear and the model incorporated parameters like the peak roughness and the height of the surface bumps, as well as a constant boundary friction coefficient that accounts for friction-modifying additives in the lubricant.

Simulation Verification and Surface Roughness Effect:

The experimental and simulation results are compared in Figure 12, where the solid black curve represents the measured torque, and the white dashed curve shows the shaft speed profile and the data used in the comparison was taken from the 3000th cycle, after the bearing had adapted to the operating conditions and the measured data show fluctuations, whereas the simulation model does not capture these variations since the shaft speed is predetermined and to evaluate the impact of surface roughness, the friction torque calculated using the worn surface roughness is compared with the new surface roughness results and the simulation shows that the friction torque at the start of rotation (breakaway torque) is primarily determined by the boundary friction coefficient, and this value remains the same regardless of whether the bearing is new or worn. In the mixed lubrication stage, where both hydrodynamic and boundary lubrication exist, the friction torque decreases rapidly, reaching a steady state once the system transitions into full hydrodynamic lubrication after 1.5 seconds and at the maximum shaft speed, the calculated torque from both new and worn surface roughness models aligns with the measured torque, indicating that the surface roughness does not significantly affect the torque during the hydrodynamic lubrication phase. However, during the deceleration phase, the simulation with the worn surface roughness results in a noticeable reduction in friction torque, better matching the measured data and the solid gray curve, representing the simulation with new surface roughness, also shows similar torque behavior during the start-stop cycle but overestimates the friction torque during the stopping phase compared to the measured data.

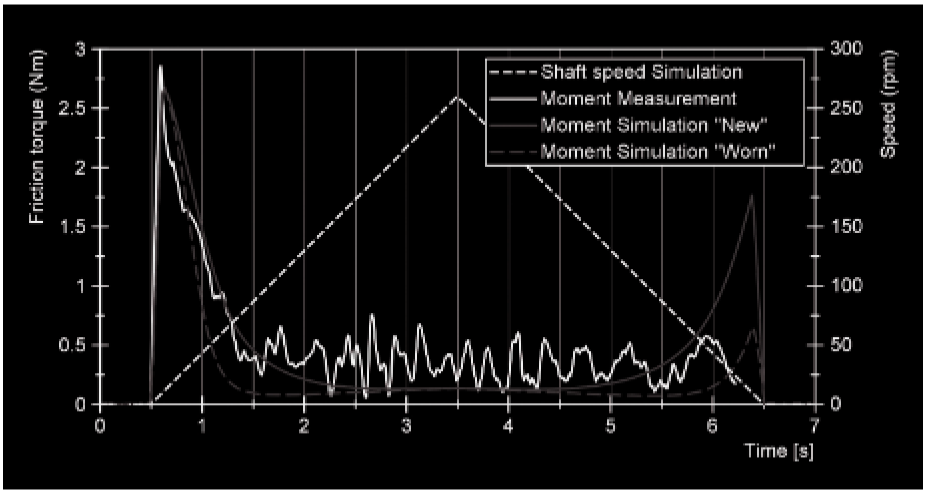

Figure 12. Comparison of Measured and Calculated Torque during a Shaft Start-Stop Cycle Using New and Worn Surface Roughness

Conclusion:

In conclusion, the research recommends the development of innovative lubricating oils that can adapt to changing operating conditions, and recommends new designs for sliding bearings that can handle high pressures and maintain proper lubrication to reduce wear and increase efficiency in internal combustion engines and this research provides an in-depth understanding of the operation of sliding bearings and their ability to meet the ongoing challenges in internal combustion engines, with the aim of improving fuel efficiency, reducing emissions, and enhancing the reliability of heavy industrial engines.

Reference

S. Bair, "Measurements of Real Non-Newtonian Response for Liquid Lubricants under Moderate Pressures," Proceedings of the Institution of Mechanical Engineers, Part J: Journal of Engineering Tribology, vol. 215, no. 3, pp. 223–233, 2001.

S. Bair, "And the Shear Rheology of Thin Compressed Liquid Films," Proceedings of the Institution of Mechanical Engineers, Part J: Journal of Engineering Tribology, vol. 216, no. 1, pp. 1–17, 2002.

S. Bair, "High Pressure Rheology for Quantitative Elastohydrodynamics," in Hydrodynamic Lubrication of Textured Surfaces: A Review of Modeling Techniques and Key Findings, D. Gropper, L. Wang, and T. J. Harvey, Eds. Tribology International, vol. 94, pp. 509–529, 2016.

M. J. Braun and W. M. Hannon, "Cavitation Formation and Modelling for Fluid Film Bearings: A Review," Proceedings of the Institution of Mechanical Engineers, Part J: Journal of Engineering Tribology, vol. 224, pp. 839–863, 2010.

Y. Qiu and M. M. Khonsari, "Experimental Investigation of Tribological Performance of Laser Textured Stainless Steel Rings," Tribology International, vol. 44, pp. 635–644, 2011.

J. Zhang and Y. Meng, "Direct Observation of Cavitation Phenomenon and Hydrodynamic Lubrication Analysis of Textured Surfaces," Tribology Letters, vol. 46, pp. 147–158, 2012.

J. George and R. Brock, "Polymeric Engine Bearings for Hybrid and Start-Stop Applications," SAE Technical Paper, 2012-01-1966, 2012.

M. Ferreira, A. Silva, M. Praça, and S. Costa, "Polymeric Coated Lead-Free Bronze Bearings for High Durability in Medium-Duty Diesel Engines," SAE Technical Paper, 2014-36-0405, 2014.

D. Gudin, O. Mian, and S. Sanders, "Experimental Measurement and Modelling of Plain Bearing Wear in Start–Stop Applications," Proceedings of the Institution of Mechanical Engineers, Part J: Journal of Engineering Tribology, vol. 227, no. 5, pp. 433–446, 2013.

G. Offner and O. Knaus, "A Generic Friction Model for Radial Slider Bearing Simulation Considering Elastic and Plastic Deformation," Lubricants, vol. 3, pp. 522–538, 2015.

K. Bobzin and T. Brögelmann, "Minimizing Frictional Losses in Crankshaft Bearings of Automobile Powertrain by Diamond-Like Carbon Coatings under Elastohydrodynamic Lubrication," Surface & Coatings Technology, vol. 290, pp. 100–109, 2015.

H. Allmaier, C. Priestner, C. Six, H. H. Priebsch, C. Forstner, and F. Novotny-Farkas, "Predicting Friction Reliably and Accurately in Journal Bearings—A Systematic Validation of Simulation Results with Experimental Measurements," Tribology International, vol. 44, pp. 1151–1160, 2011.

C. Priestner, H. Allmaier, H. H. Priebsch, and C. Forstner, "Refined Simulation of Friction Power Loss in Crankshaft Slider Bearings Considering Wear in the Mixed Lubrication Regime," Tribology International, vol. 46, no. 1, pp. 200–207, 2012.

N. Patir and H. Cheng, "An Average Flow Model for Determining Effects of Three-Dimensional Roughness on Partial Hydrodynamic Lubrication," ASME Journal of Lubrication Technology, vol. 100, pp. 12–17, 1978.

N. Patir and H. Cheng, "Application of Average Flow Model to Lubrication Between Rough Sliding Surfaces," ASME Journal of Lubrication Technology, vol. 101, no. 2, pp. 220–229, 1979.

G. Offner, "Friction Power Loss Simulation of Internal Combustion Engines Considering Mixed Lubricated Radial Slider, Axial Slider, and Piston to Liner Contacts," Tribology Transactions, vol. 56, no. 3, pp. 503–515, 2013.

M. O. A. Mokhtar, R. B. Howarth, and P. B. Davies, "Wear Characteristics of Plain Hydrodynamic Journal Bearings During Repeated Starting and Stopping," Tribology Transactions, vol. 20, no. 3, pp. 191–194, 1977.

M. Wilcutts, J. Switkes, M. Shost, and A. Tripathi, "Design and Benefits of Dynamic Skip Fire Strategies for Cylinder Deactivated Engines," SAE Technical Paper, 2013-01-0359, 2013.

M. Mohammadpour, R. Rahmani, and H. Rahnejat, "The Effect of Cylinder De-Activation on Thermo-Friction Characteristics of the Connecting Rod Bearing in the New European Drive Cycle (NEDC)," SAE Technical Paper, 2014-01-2089, 2014.

M. Mohammadpour, R. Rahmani, and H. Rahnejat, "Effect of Cylinder Deactivation on the Tribo-Dynamics and Acoustic Emission of Overlay Big End Bearings," Proceedings of the Institution of Mechanical Engineers, Part K: Journal of Multi-Body Dynamics, vol. 228, no. 2, pp. 138–151, 2014.

H. Shahmohamadi, R. Rahmani, H. Rahnejat, C. P. Garner, and D. Dowson, "Big End Bearing Losses with Thermal Cavitation Flow under Cylinder Deactivation," Tribology Letters, vol. 57, no. 2, pp. 1–17, 2015.

K. Holmberg, P. Andersson, N. O. Nylund, K. Mäkelä, and A. Erdemir, "Global Energy Consumption Due to Friction in Trucks and Buses," Tribology International, vol. 78, pp. 94–114, 2014.

J. L. Ligier and B. Noel, "Friction Reduction and Reliability for Engine Bearings," Lubricants, vol. 3, pp. 569–596, 2015.

V. Macián, B. Tormos, V. Bermúdez, and L. Ramírez, "Assessment of the Effect of Low Viscosity Oils Usage on a Light Duty Diesel Engine Fuel Consumption in Stationary and Transient Conditions," Tribology International, vol. 79, pp. 132–139, 2014.

V. Macián, B. Tormos, S. Ruiz, and G. Miró, "Low Viscosity Engine Oils: Study of Wear Effects and Oil Key Parameters in a Heavy-Duty Engine Fleet Test," Tribology

International, vol. 94, pp. 240–248, 2016.

H. Allmaier, C. Priestner, F. M. Reich, H. H. Priebsch, C. Forstner, and F. Novotny-Farkas, "Predicting Friction Reliably and Accurately in Journal Bearings—The Importance of Extensive Oil-Models," Tribology International, vol. 48, pp. 93–101, 2012.